https://doi.org/10.48048/tis.2022.6181

Characterization of Pure and L-Proline Doped Potassium Nitrate and Sodium Nitrate Crystals

Mathivanan Velumani[1], Prince Makarios Paul[2], Muthiah Haris[2,*], Muthuswamy Senthilkumar[2], Abiram Angamuthu[2] and Chandrasekaran Joseph[3]

[1]Department of Physics, Nehru Institute of Engineering and Technology, Tamil Nadu 641105, India
[2]Department of Physics, Karunya Institute of Technology and Sciences, Tamil Nadu 641114, India
[3]Department of Physics, Sri Ramakrishna Mission Vidyalaya College of Arts and Science, Coimbatore 641020, India

([*]Corresponding author's e-mail: harismuthiah@gmail.com)

Received: 6 July 2021, Revised: 16 September 2021, Accepted: 23 September 2021

Abstract

The crystals of pure and L-Proline doped Potassium nitrate and Sodium nitrate were grown in solution by slow evaporation technique using supersaturated solution of the salts. Characterization studies of the crystals have been done to find the impact of the L-Proline on the regular lattice arrangement of the pure crystal. The Powder XRD spectrum reveals that the pure and doped KNO_3 crystals belong to orthorhombic structure; and pure and doped $NaNO_3$ are rhombohedral in nature. This is a unit cell with parameters $\mathbf{a = b = c;\ \alpha = \beta = \gamma \neq 90°}$. There are small changes in the unit cell dimensions but the structure of the pure and doped crystals remain to be orthorhombic in nature. The FTIR spectrum shows the functional group analysis of the samples. The various decomposition process of the crystals with respect to temperature have been carried out in thermal analysis. The dielectric properties exhibit the variation of dielectric constant, and capacitance with frequency at various temperatures for pure and doped crystals. The doped crystals found to have considerable effect on the optical, thermal and dielectric properties.

Keywords: Dielectric studies, Doped KNO_3 and $NaNO_3$, Powder XRD, FTIR, Thermal analysis

Introduction

Focus of research in solid state ionics is gaining importance in recent past because of their potential applications in various solid-state devices [1,2]. This field involves mainly the study of transport phenomena of ions in solids. The study of ionic conductivity exhibits special role in knowing the lattice defects and energy for defects in the structure of crystals. Solid state ionics was first studied in crystalline solid electrolytes, but as time went on, the field extended to include polycrystalline, glassy, mixed, and dispersed solid electrolyte systems. Conduction owing to ion migration in solid electrolytes is negligible at ambient temperature but significant at high temperatures. The researchers were inspired to develop novel solid electrolytes by applying various ways of synthesis to increase the ionic conduction in these solid electrolytes due to the growing demand for alternative power sources, high energy storage devices, and energy conversion systems. However, earlier investigations show that the enhancement of conductivity is not much appreciable by the method of conventional doping [3].

A good amount of work has already been reported on Lithium and Sodium based solid electrolyte systems [4,5]. AC and DC conductivity studies on dispersed and polymer sodium electrolyte systems revealed appreciable enhancement of ionic conductivity [6,7]. A series of pure and mixed crystals have been studied by several researchers with the aim of identifying new materials [8-10]. Electrical, dielectrical, and micro-hardness studies on mixed crystals of alkali and alkaline earth halides, such as KCl - NaCl, KBr - KI, KCl - KBr, KBr - NaI, AgBr - AgCl, and CaF_2 - SrF_2 have been reported extensively [11-14]. A normal Na + ionic conductor, $NaNO_3$ has been chosen and an attempt has been made to improve the conductivity by mixing with $Sr(NO_3)_2$, another solid ionic conductor, heterogeneously. An enhancement in ionic conductivity has been revealed in the study of ionic transport in $Sr(NO_3)_2$ dispersed with Al_2O_3 [15,16]. In the case of L-proline doped potassium dihydrogen phosphate (KDP) single crystals, due to variation in the doping concentration, there is a modification in the growth habit,

nonlinear optical property and mechanical hardness of the doped crystals. SHG studies have shown an enhancement in the NLO property due to doping. Mechanical hardness of the crystal also depends on the concentration of the dopant.

Purpose of this work is to grow extremely pure potassium nitrate and sodium nitrate crystals by using L-Proline as a dopant. Such highly pure crystals of potassium nitrate and sodium nitrate were subjected to different studies including Optical properties, thermal analysis and dielectric properties.

Materials and methods

The commercially available chemicals of pure KNO_3, L-Proline doped KNO_3, pure $NaNO_3$, L-Proline doped $NaNO_3$ (with 99.9 % Purity) were taken in different mole ratios and grown them as single crystals by using slow evaporation method. The supersaturated solution of L-Proline doped KNO_3 and L-Proline doped $NaNO_3$ has been prepared and placed in a petri dish. Crystals of high quality have been synthesized. The grown single crystals are shown in Figure 1. The grown crystals were orthorhombic in structure.

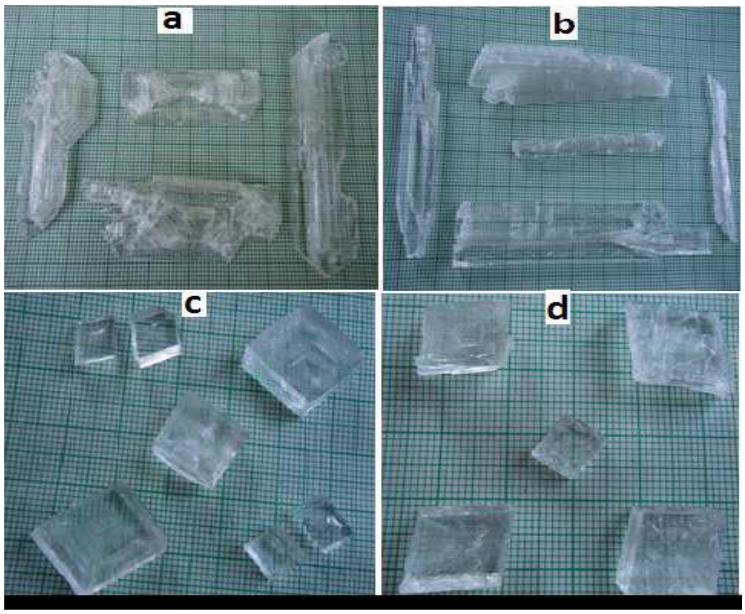

Figure 1 Crystals of (a) pure KNO_3 (b) L-Proline doped KNO_3 (c) pure $NaNO_3$ (d) L-Proline doped $NaNO_3$.

Results and discussion

Powder XRD studies

The grown crystals were characterized by powder xray diffraction using a Bruker D8 Advance, Germany instrument with CuKα radiation (1.5406 Å). The sample was scanned in the range 5 - 70° at the scan rate of 1° min^{-1}. X-ray diffraction is based on constructive interference of monochromatic X-rays and a crystalline sample. These X-rays are generated by a cathode ray tube, filtered to produce monochromatic radiation, collimated to concentrate, and directed toward the sample. The interaction of the incident rays with the sample produces constructive interference (and a diffracted ray) when conditions satisfy Bragg's Law ($n\lambda=2d \sin\theta$). The powder XRD analysis for the grown crystals has been carried out to identify the lattice parameters. The cell parameters of the grown pure KNO_3 were found to be a = 6.787 Å, b = 8.995 Å, c = 5.892 Å. The cell parameters of L-Proline doped KNO_3 is found be a = 6.717 Å, b = 8.908 Å, c = 5.270Å. Both pure and doped crystal belongs to orthorhombic symmetry. Similarly, the calculated lattice parameters for pure $NaNO_3$ are; a = 14.793 Å, b = 5.2834 Å, c = 9.234 Å and for L-Proline doped $NaNO_3$ are; a = 14.910 Å, b = 5.783 Å, c = 8.238 Å. The crystal belongs to rhombohedral structure with space group D_2. XRD patterns of the systems, as shown in **Figures 2** and **3** reveals that there are new peaks which shows that the dopant L-Proline has entered the lattice of pure crystals.

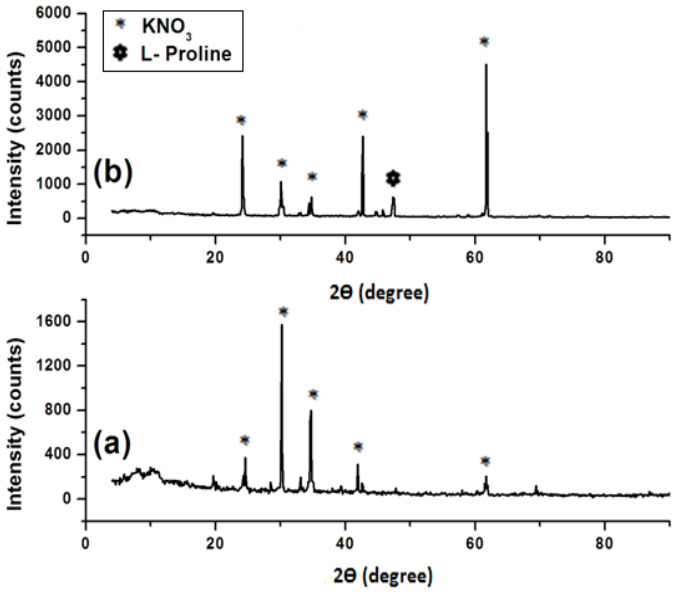

Figure 2 Powder XRD of (a) pure and (b) L-Proline doped KNO_3.

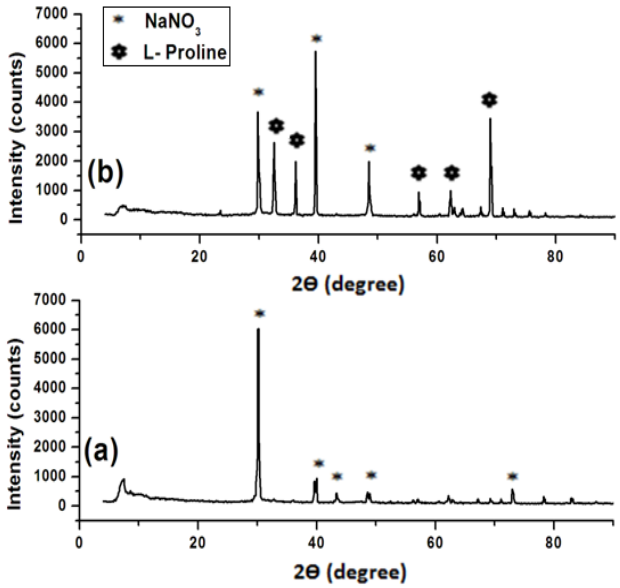

Figure 3 Powder XRD of (a) pure and (b) L-Proline doped $NaNO_3$.

FTIR spectroscopy

The Fourier Transform infrared spectrum was recorded for powdered samples of pure and L-proline doped Potassium and Sodium Nitrate crystals using Perkin-Elmer FTIR spectrometer by KBr pellet technique in the range 400 - 4,000 cm^{-1}. The infrared radiations promotes transitions in a molecule between rotational and vibrational energy levels of the ground electronic energy state. The FTIR spectra of pure and L-proline added Potassium and Sodium nitrate crystals are shown in **Figure 4**. If peak shift is towards higher wave number side, mass of that molecule is reduced. Because frequency of vibration is inversely proportional to mass of vibrating molecule. so lighter the molecule, more the vibration frequency and higher the wave numbers. The addition of L-proline brought changes in the intensity of peaks in doped crystals. The peaks at 1,761 and 1,795 cm^{-1} in pure KNO_3 and $NaNO_3$ shows the symmetric stretching mode of NO_2. These peaks are shifted to 1,768 and 1,787 cm^{-1}, respectively in

doped crystals. The peaks at 2,070 and 2,098 cm^{-1} in pure KNO_3 and $NaNO_3$, respectively, shows the asymmetric stretching mode of NO_2. These peaks are shifted to 2,065 and 2,102 cm^{-1}, respectively in the doped crystals. The sharp peaks at 2,389 and 1,795 cm^{-1} of pure crystals assigned as NH_3^+ and C=O stretching vibrations are shifted to 2,396 and 1,787 cm^{-1}, respectively. The symmetric stretching vibration of NH_3^+ at 2,471 cm^{-1} and C-C stretching group at 827 cm^{-1} [17-20] are shifted to 2,485 and 836 cm^{-1} due to doped of L-proline. Also, the shifted peaks are observed in **Figures 4(b)** - **4(d)** are confirmed the doped of L-proline.

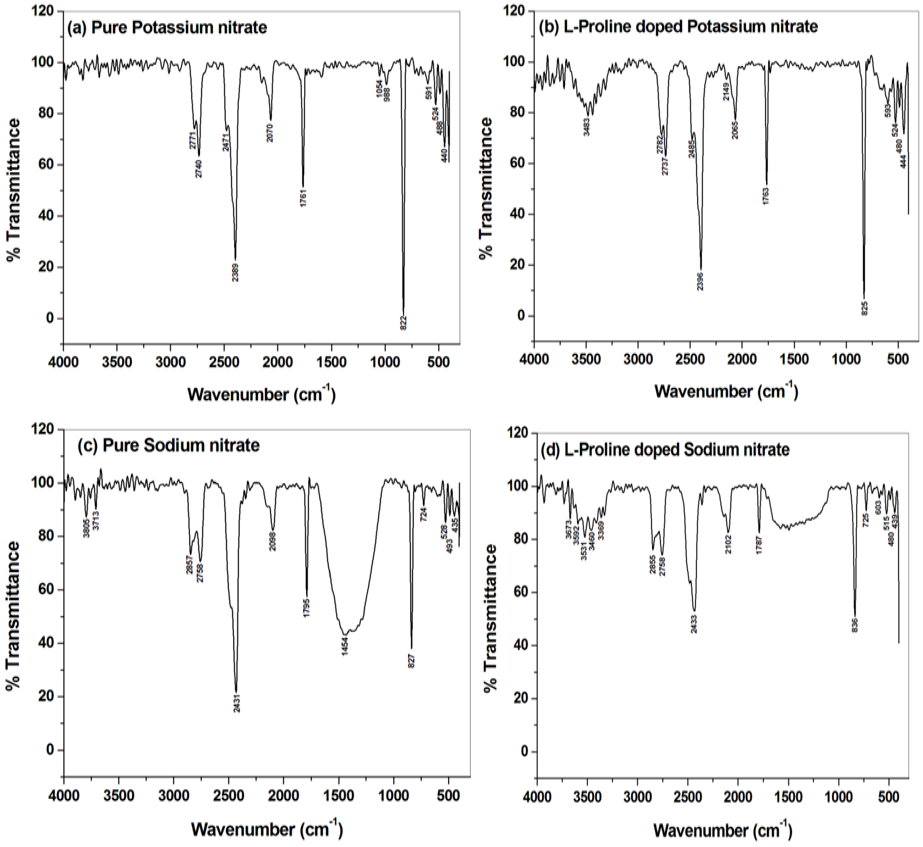

Figure 4 FTIR spectrum for pure and L-Proline doped KNO_3 and $NaNO_3$.

Thermal analysis

The basic instrumental requirements for TGA are a precision balance with a pan loaded with the sample, and a programmable furnace. The furnace can be programmed either for a constant heating rate, or for heating to acquire a constant mass loss with time. Differential scanning calorimetry can be used to measure a number of characteristic properties of a sample. Using this technique it is possible to observe fusion and crystallization events as well as glass transition temperatures TG. The TGA and DSC curves of pure and L-Proline doped KNO_3 and $NaNO_3$ crystals are shown in **Figure 5**. There are major stages of decomposition in the pure and doped Potassium nitrate crystals. This can be observed through the TG curve. In the pure Potassium nitrate, the first, second and third stages of decomposition take place from 36 - 260 °C with a loss of weight of 60 %, 265 - 619 °C with a loss of weight of 20 % and 635 - 700 °C with a loss of weight of 20 %, respectively. Thus, in this temperature range of 36 - 700 °C, the material gets completely decomposed. In the L-Proline doped Potassium nitrate, the first, second and third stages of decomposition takes place from 36 - 610 °C with a loss of weight of 10 %, 615 - 865 °C with a loss of weight of 70 % and 870 - 1,000 °C with a loss of weight of 8 %, respectively. Thus in this temperature range of 36 - 1000 °C, the material doesn't get decomposed completely.

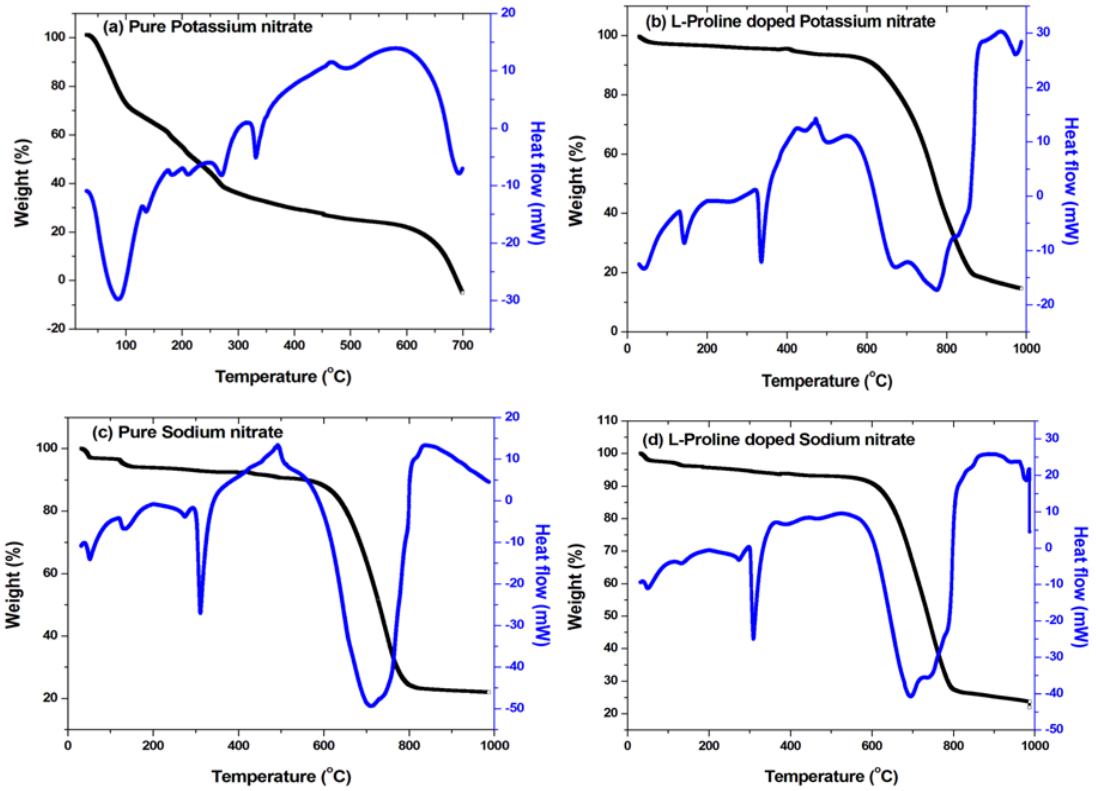

Figure 5 TG analysis of pure and L-Proline doped KNO_3 and $NaNO_3$.

There are 2 major stages of decomposition in the pure and doped Sodium nitrate crystals. This can be observed through the TG curve. In the pure Sodium nitrate, the first and second stages of decomposition takes place from 36 - 603 °C with a loss of weight of 10 % and 605 - 1,000 °C with a loss of weight of 71 %, respectively. Thus, in this temperature range of 36 - 1,000 °C, the material doesn't get completely decomposed. In the L-Proline doped Sodium nitrate, the first and second stages of decomposition takes place from 36 - 603 °C with a loss of weight of 8 % and 605 - 1,000 °C with a loss of weight of 72 %, respectively. Thus, in this temperature range of 36 - 1,000 °C, the material doesn't get decomposed completely.

Dielectric studies

Dielectric properties of the crystals are related mutually with electro-optic property of the crystals: Especially when the conducting materials are not present [18]. The dielectric studies were measured for pure, and L-proline doped sodium nitrate and potassium nitrate crystal. The dielectric constant was calculated by using the relation $\varepsilon_r = Cd/\varepsilon_o A$, where C = capacitance of sample, d = thickness of sample, A = area of sample and ε_o = absolute permittivity.

In the present investigation, the dielectric analysis of crystals was taken by using HIOKI 3532-50 LCR hitestester instrument and a conventional sample holder (westphal). In order to ensure good electrical contact between the sample and the electrodes, silver paint was applied to the surfaces of the samples.

Figures 6(a) - 6(d) show the variation of dielectric constant with respect to frequency for different temperatures for both pure and L-proline doped KNO_3 and $NaNO_3$ crystals. The dielectric constants were measured for various temperatures (28 - 120 °C) with variation of frequency of applied field. The dielectric constant decreases speedily as frequency increases and ε_r increases along with the increase in temperature. The higher value of dielectric constant at low frequency is due to the existence of space charge polarization near the grain boundary interfaces, which depends on the perfection and purity of the sample [19]. At lower frequencies, the dipoles can easily change alignment with the switching field. As the frequency gets increases, the dipoles rotate less and do not maintain phase with the applied filed and hence reduce their contribution towards polarization.

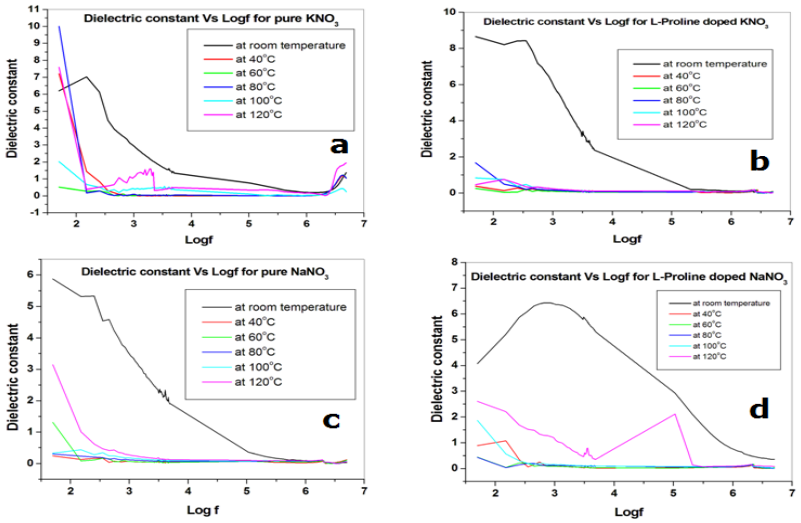

Figure 6 Dielectric constant vs frequency for pure and L-Proline doped potassium and sodium nitrate at various temperature.

It is also clear in **Figures 6(b) - 6(d)**, the L-proline doped KNO_3 and $NaNO_3$ concentration affects the values of dielectric constants at various temperatures. As the doped level, the rapid decreases in the values of the dielectric constant with increase in the frequency of the applied field and ε_r decreases along with increase temperatures suggest that the dipoles cannot comply with the changes in the frequency of the applied field after the certain value.

Figures 7(a) - 7(d) give the changes in resistivity with the frequency with respect to different temperatures for both pure and L-proline doped KNO_3 and $NaNO_3$ crystals. The resistivity and conductivity were found out by using the following formula: $\rho = A/2\pi fCd$, $\sigma = 1/\rho$, where C - is the capacitance, d is the thickness, A is the area of the crystal, and f is the frequency of the applied field. From the **Figures 7(a) - 7(c)**, it is observed that the resistance of pure $NaNO_3$ and KNO_3 decreased rapidly as frequency increased. But the value of resistance is increased with temperature increases. This may be due to the shift of the dielectric transition towards lower temperatures for the single crystal and the difference in absolute values of electrical resistance related to the presence of the inter-crystallite boundaries in the single crystal.

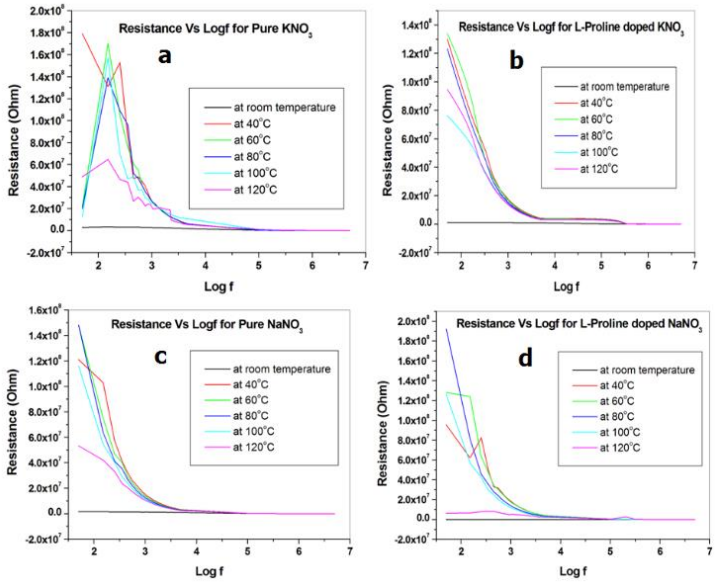

Figure 7 Resistance vs frequency for pure and L-Proline doped potassium and sodium nitrate at various temperature.

The resistance of doped L-proline $NaNO_3$ and KNO_3 are shown in Fig. 8b and 8d. The resistance of doped crystal is known to decrease along with frequency increases. The resistance of doped crystal increases with the temperature increases due to the reduced number of grain boundaries [20]. The resistance of both doped crystal is slightly higher than in both pure crystalline materials. The lowered resistance of grown crystal at the room temperature reflects the fact that the doped impurities did not contribute to electron-impurity scattering.

The variation in capacitance with the frequency for the various temperatures for both pure and L-proline doped KNO_3 and $NaNO_3$ crystals are shown in **Figures 8(a) - 8(d)**. The pure crystal shows the capacitance of all the grown crystals decreases with increase in temperature and frequency.

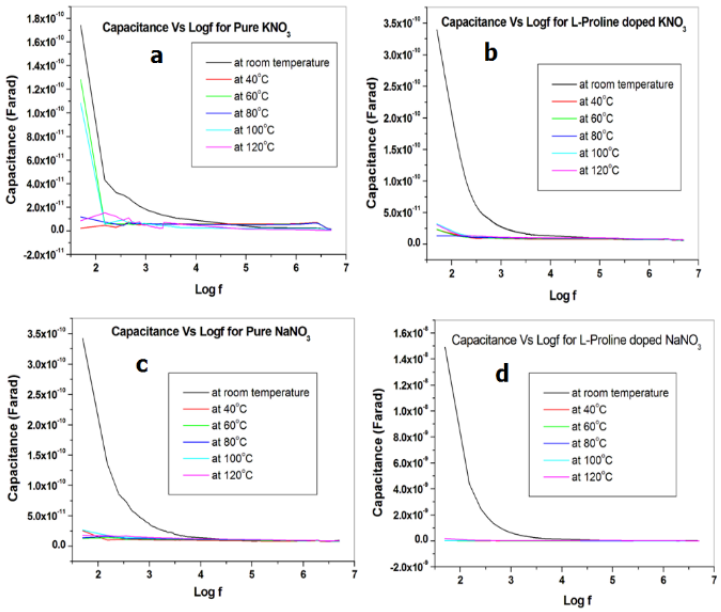

Figure 8 Capacitance vs frequency for pure and L-Proline doped potassium and sodium nitrate at various temperature.

But in doped region, the plotted graphs it can be noted that capacitance decreases only in room temperature and the value of capacitance are nearly constant with increase in temperature and frequency. Also, this plotted graph shows higher capacitance values at low frequency range similar that of dielectric constant. So, they are limited to low frequency applications due to lower dielectric constant and capacitance losses at higher frequencies. The results show that the grown crystal having a good dielectric constant, resistance, and capacitance due to the L-proline doped with $NaNO_3$ and KNO_3 [21-24].

Conclusions

The pure and L-Proline doped Potassium nitrate and Sodium nitrate crystals were grown in solution by slow evaporation technique.

1) The Powder XRD spectrum reveals that the unit cell volume of pure and doped KNO_3 to be 359.700Å^3 and 315.330Å^3, respectively; and for pure and doped $NaNO_3$ is found to be 721.704Å^3 and 710.317Å^3.

2) The functional group analysis from the FTIR spectrum reveals that the dopant L-Proline has entered the lattice of doped crystals.

3) The TGA and DSC analysis confirms that there is water of hydration since there is loss of weight around 100 °C.

4) The variation of dielectric constant, resistance, and capacitance with respect to frequency at various temperatures reveals that the dopant L-Proline has a significant effect on the pure crystals.

The grown L-Proline doped KNO3 and L-Proline doped NaNO3 crystals can be used to find the difference in refractive index property, Mechanical strength and NLO properties which plays a vital role in the research industry.

Acknowledgements

The author J. Chandrasekaran gratefully acknowledges the instrumental support from the DST, Government of India, for the major research project (SB/EMEQ-293/2013).

References

[1] Z Liu, S Ma, J Liu, S Xiong, Y Ma and H Chen. High ionic conductivity achieved in $Li_3Y(Br_3Cl_3)$ mixed halide solid electrolyte via promoted diffusion pathways and enhanced grain boundary. *ACS Energy Lett.* 2021; **6**, 298-304.

[2] M Moriya, D Kato, W Sakamoto and T Yogo. Structural design of ionic conduction paths in molecular crystals for selective and enhanced lithium-ion conduction. *Chem. Eur. J.* 2013; **19**, 13554.

[3] N Sinha, N Goel, BK Singh, MK Gupta and B Kumar. Enhancement in ferroelectric, pyroelectric and photoluminescence properties in dye doped TGS crystals. *J. Solid State Chem.* 2012; **190**, 180-5.

[4] DR MacFarlane, J Huang and M Forsyth. Lithium-doped plastic crystal electrolytes exhibiting fast ion conduction for secondary batteries. *Nature* 1999; **402**, 792-4.

[5] A Dey, S Karan and SK De. Molecular interaction and ionic conductivity of polyethylene oxide-LiClO4 nanocomposites. *J. Phys. Chem. Solid.* 2010; **71**, 329-35.

[6] N Ennaceur, K Jarraya, A Singh, I Ledoux-Rak and T Mhiri. Phase transitions, ferroelectric behavior and second-order nonlinear optics of a new mixed sodium dihydrogen phosphate-arsenate. *J. Phys. Chem. Solid.* 2012; **73**, 418-22.

[7] KM Zaidan, RA Talib, MA Rahma and FH Khaleel. Synthesis and characterization of poly (o-toluidine) POT blend with polyethylene oxide PEO as conducting polymer alloys. *Chem. Sin.* 2012; **3**, 841-8.

[8] MV MadhavaRao, SN Reddy and AS Chary. DC ionic conductivity of $NaNO_3$: γ- Al_2O_3 composite solid electrolyte system. *Phys. B Condens. Matter* 2005; **362**, 193-8.

[9] AA Zakariah, AD Folorunsho, AY Mariam and K Yakaka. Evaluation of selected halogen anions for the elongation of Leclanche cell's lifespan. *Adv. Appl. Sci. Res.* 2012; **3**, 280-98.

[10] P Shenoy, KV Bangera and GK Shivakumar. Growth and thermal studies on pure ADP, KDP and mixed $K_{1-x}(NH_4)_{xH2}PO_4$ crystals. *Cryst. Res. Tech.* 2010; 45, 825-9.

[11] K Rajesh and PP Kumar. Mechanical, thermal, linear and nonlinear optical properties of barium L-tartrate single crystal. *Mater. Res. Express* 2017; **4**, 016502.

[12] A Tiwari, NK Gaur and RK Singh. Anomalous thermoelastic behaviour of orientationally disordered $(NH_4I)_x(KI)_{1-x}$ mixed crystals. *J. Phys. Chem. Solid.* 2010; **71**, 717-21.

[13] P Gao, M Gu, X Lin-Liu, H Shi-Ming, B Liu, C Ni, X Rong-Kun and N Jia-Min. The influence of concentration and super saturation ratio of CuI-HI on CuI crystal growth by decomplexation method. *Cryst. Res. Tech.* 2008; **45**, 365-70.

[14] T Zhang, M Yang, EE Benson, Z Li, JVD Lagemaat, JM Luther, Y Yan, K Zhu and Y Zhao. A facile solvo thermal growth of single crystal mixed halide perovskite $CH_3NH_3Pb(Br_{1-x}Cl_x)_3$. *Chem. Comm.* 2015; **51**, 7820-3.

[15] T Kawai, Y Sugata and S Shimanuki. Jahn-teller effect of Au− centers in KCl_xBr_{1-x} mixed crystals. *J. Lumin.* 2000; **87-89**, 636-8.

[16] LA Akhmedova-Azizova. Thermal conductivity and viscosity of aqueous of $Mg(NO_3)_2$, $Sr(NO_3)_2$, $Ca(NO_3)_2$, and $Ba(NO_3)_2$ solutions. *J. Chem. Eng. Data* 2006; **51**, 2088-90.

[17] SK Arora, V Patel, B Amin and A Kothari. Dielectric behaviour of strontium tartrate single crystals. *Bull. Mater. Sci.* 2004; **27**, 141-7.

[18] S Aruna, G Bhagavannarayana, M Palanisamy, PC Thomas, B Varghese and P Sagayaraj. Growth, morphological, mechanical, and dielectric studies of semi organic NLO single crystal: L-argininium perchlorate. *J. Cryst. Growth* 2007; **300**, 403-8.

[19] JY Kim, O Min-Wook, S Lee, YC Cho, Y Jang-Hee, GW Lee, C Chae-Ryong, CH Park and J Se-Young. Abnormal drop in electrical resistivity with impurity doping of single-crystal Ag. *Sci. Rep.* 2014; **4**, 5450.

[20] E Gallegos-Loya and JA Duarte-Moller. Physico-chemical properties of alanine-sodium nitrate: An optical overview. *Int. J. Phys. Sci.* 2011; **6**, 3310-8.

[21] PL Praveen and DP Ojha. Photosensitivity, substituent and solvent-induced shifts in UV-visible absorption bands of naphthyl-ester liquid crystals: A comparative theoretical approach. *Liq. Cryst.* 2014; **41**, 872-82.

[22] PL Praveen and DP Ojha. Calculation of spectral shifts in UV-visible region and photoresponsive behaviour of fluorinated liquid crystals: Effect of solvent and substituent. *Mater. Chem. Phys*. 2014; **135**, 628-34.
[23] PL Praveen and DP Ojha. Calculation of spectral shifts in UV-visible region and photo stability of thermotropic liquid crystals: Solvent and alkyl chain length effects. *J. Mol. Liq*. 2012; **169**, 110-6.
[24] PL Praveen, DS Ramakrishna and DP Ojha. UV spectral characterization of a smectic-C liquid crystal: Theoretical support to the experiment. *Mol. Cryst. Liq. Cryst*. 2017; **643**, 76-82.